Strain and spin-orbit coupling induced orbital ordering in the Mott insulator $BaCrO_3$

Hyo-Sun Jin,[1] Kyo-Hoon Ahn,[1] Myung-Chul Jung,[1] and K.-W. Lee[1,2]
[1]*Department of Applied Physics, Graduate School, Korea University, Sejong 339-700, Korea*
[2]*Department of Display and Semiconductor Physics, Korea University, Sejong 339-700, Korea*
(Received 28 April 2014; revised manuscript received 24 August 2014; published 18 November 2014)

Using *ab initio* calculations, we have investigated an insulating tetragonally distorted perovskite $BaCrO_3$ with a formal $3d^2$ configuration, the volume of which is apparently substantially enhanced by a strain due to $SrTiO_3$ substrate. Inclusion of both correlation and spin-orbit coupling (SOC) effects leads to a metal-insulator transition and in-plane zigzag orbital ordering (OO) of alternating singly filled $d_{xz} + id_{yz}$ and $d_{xz} - id_{yz}$ orbitals, which results in a large orbital moment $M_L \approx -0.78\mu_B$ antialigned to the spin moment $M_S \approx 2|M_L|$ in Cr ions. Remarkably, this ordering also induces a considerable M_L for apical oxygens. Our findings show metal-insulator and OO transitions, driven by an interplay among strain, correlation, and SOC, which is uncommon in $3d$ systems.

DOI: 10.1103/PhysRevB.90.205124 PACS number(s): 71.20.Be, 71.20.Dg, 71.30.+h, 75.50.Ee

I. INTRODUCTION

In condensed matter physics the interplay among strain, strong correlation, and spin-orbit coupling (SOC) has been becoming extremely important [1–3]. This leads to abundant unconventional phenomena such as magnetic ordering, interface superconductivity, metal-insulator transitions, and more recently topological insulators [4–10]. In a Mott transition, in particular, the ratio U/W of correlation strength U to bandwidth W determines charge, spin, and orbital orderings. W can be controlled by external factors such as doping, pressure, and strain by a proper choice of substrate. The strain has been of great interest for applications of band engineering [4–8]. Recently, another type of the Mott insulator induced by correlation effects which are assisted by spin-orbit coupling (SOC), named relativistic Mott insulator, has been observed in cubic double perovskite Ba_2NaOsO_6 and a few Ir-based oxides, which show substantially strong SOC [11,12]. The relativistic Mott transition was also proposed to occur even in the $4d$ Li_2RhO_3 system [13]. In this transition, SOC leads to the removal of degeneracy in partially filled bands or narrowing of the bandwidth, and then strong correlation selects a filled orbital. However, pure correlation effects often lead to a metal-insulator transition in $3d$ systems, where the strength of SOC is negligible compared to that of correlation. Here, we will address a strain and SOC-driven Mott transition, accompanied by orbital ordering (OO), in the $3d^2$ $BaCrO_3$ thin film synthesized recently [14]. In this system, strength of SOC is indeed tiny, but crucial to open a gap. This has been rarely observed in $3d$ systems.

Tetravalent d^2 chromate perovskites have recently drawn attention due to their atypical and controversial properties [15–19]. Although the orthorhombic antiferromagnet $CaCrO_3$ is metallic, it was suggested that correlation effects play an important role [15,16]. Another metallic antiferromagnet $SrCrO_3$ has a tetragonally distorted structure due to partial OO of $(d_{xy})^1(d_{xz}d_{yz})^1$ [17,18]. Through correlated first principles calculations, Gupta *et al.* proposed that lattice distortions in an ultrathin $SrCrO_3$ film lead to OO, which in turn induces ferroelectricity [19]. Recently, Zhu *et al.* synthesized the missing member, $BaCrO_3$, of the tetravalent chromate perovskites, on $SrTiO_3$ (001) surfaces [14]. As observed in the isostructural $SrCrO_3$ [17], the distortion factor of a/c is as small as approximately 0.5%, and this prevents the CrO_6 octahedron from rotating and tilting (see below). The magnetic measurements show hysteresis with a small coercive field and small saturated moment of $0.028\mu_B$ with Curie temperature $T_C = 25$ K, indicating a weak ferromagnet (FM) or canted antiferromagnet (AFM). The resistivity data follow an insulating behavior with a kink at $T \approx 200$ K and indicate an activation energy gap of ~0.38 eV. They also performed correlated first principles calculations using the local spin density approximation plus Hubbard U (LSDA + U) approach, but failed to obtain the observed insulating state [14]. Motivated by the failure of LSDA + U, Giovannetti *et al.* carried out dynamical mean field calculations and concluded that a Jahn-Teller distortion in the plane of the tetragonal cell with two different Cr-O bond lengths would lead to an insulating state [20].

The nature of the insulating state of $BaCrO_3$ can be unveiled from first principles calculations, including U and (relativistic) SOC effects, using an accurate all-electron full-potential electronic method of WIEN2K [21]. Considering only U and SOC simultaneously throughout the LSDA + SOC + U approach, we obtained the experimentally observed insulating state [14], indicating a crucial role of SOC. In contrast to the Jahn-Teller distortion incorporated scenario [20], our results show that this insulating state is induced by the small structure distortion and SOC activated by narrowing W, resulting from the enlarged volume due to the strain of the substrate. The accompanying OO stabilizes the C-type AFM (C-AFM), which is antiparallel in-plane and parallel along the c axis, and leads to an unusually large orbital moment M_L equal to half of the spin moment M_S in this system. Interestingly, as shown below, this feature also drives a considerable M_L in the apical oxygens.

II. CRYSTAL STRUCTURE AND CALCULATION METHOD

According to the experiment by Zhu *et al.*, the tetragonal perovskite phase appears to be unstable in the bulk [14]. We optimized the crystal structure to investigate stability of the tetragonal structure. During the optimization in the tetragonal phase, the ratio a/c was fixed at the value obtained in the experiment [14]. The structural parameters were optimized until forces were smaller than 2 mRy/a.u. As shown in

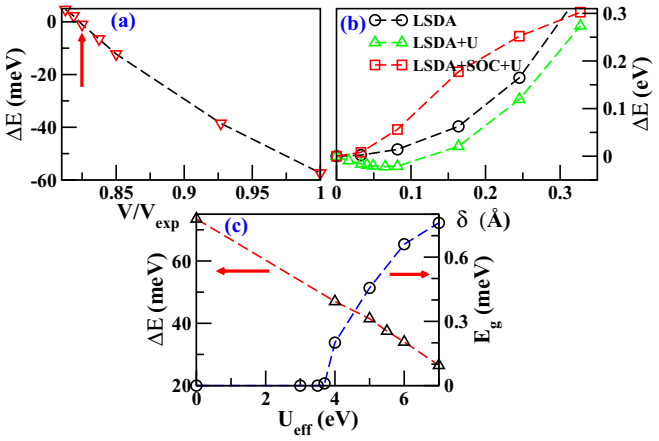

FIG. 1. (Color online) (a) Difference in energy between the cubic and the tetragonal phases, as a function of volume. The arrow denotes the optimized volume. (b) Change in energy versus a variation of the in-plane Jahn-Teller distortion δ. Here δ is the difference between short and long Cr-O bond lengths. The results of LSDA + SOC, very similar to those of LSDA, are not shown here. The Jahn-Teller distortion is only stable in the LSDA + U calculations. (c) Energy difference between FM and C-AFM (left side), and the energy gap (right side) as a function of the effective Coulomb repulsion U_{eff} in LSDA + SOC + U.

Fig. 1(a), our optimized volume is about 18% less than that of the experiment. Considering that the L(S)DA usually underestimates an experiment volume by at most several percent, as observed for the similar compound $SrCrO_3$ [18], this difference is significant. This implies that the $SrTiO_3$ substrate significantly expands the volume of $BaCrO_3$, consistent with the instability of the bulk state [14]. Remarkably, near the optimized volume the cubic and tetragonal phases are nearly degenerate. We will return to this issue below. When c-axis lattice parameter in perovskites decreases, the in-plane lattice parameter tends to increase to prevent the volume from varying [22]. This leads to the distortion from the cubic to the tetragonal structures. For the experiment volume, the tetragonal phase has an energy 57 meV lower than the cubic phase, consistent with the experiment. We also investigated a possible tilting and rotating of the CrO_6 octahedron. However, our trials to obtain this gadolinium orthoferrite $GdFeO_3$-type structure always converged to the tetragonal phase observed in the experiment [14], indicating that the $GdFeO_3$-type distortion is not energetically favored in this system. From hereon, unless stated otherwise, we use the experiment lattice parameters $a = 4.09$ Å and $c = 4.07$ Å [14].

In WIEN2K, the basis size was determined by $R_{mt} K_{\max} = 7$ and augmented-plane-wave sphere radii (2.5 for Ba, 2.01 for Cr, and 1.82 for O). The Brillouin zone was sampled with up to a dense k mesh of $11 \times 11 \times 15$. Additionally, linear response full-phonon calculations were performed with QUANTUM ESPRESSO [23]. These calculations were carried out with a $2 \times 2 \times 2$ q mesh, a $14 \times 14 \times 14$ k mesh, an energy cutoff of 40 Ry, and a charge cutoff of 400 Ry.

III. RESULTS

The results of the generalized gradient approximation plus Hubbard U (GGA + U), performed by Giovannetti *et al.* [20], show that the in-plane Jahn-Teller distortion is stable. This is consistent with our LSDA + U calculations, as shown in Fig. 1(b). However, the addition of SOC to the LSDA + U approach relieves the Jahn-Teller distortion in both metallic and insulating states. This rules out the scenario of Mott transition driven by the Jahn-Teller distortion in this system, which was proposed by Giovannetti *et al.*

In the CrO_6 octahedron, the tetragonal distortion, shortening of c lattice parameter, lowers the center of d_{xy} and results in the splitting of the t_{2g} manifold into the singlet d_{xy} and doublet d_{xz}/d_{yz}. Thus, for this d^2 configuration, the doublet is half-filled in a spin ordered state.

Initially, we applied the on-site Coulomb repulsion U to the Cr ions to obtain the observed insulating state, using the LSDA + U approach, in which the effective on-site Coulomb repulsion $U_{\text{eff}} = U - J$ was used where J is the Hund's exchange integral. As observed in the previous calculation [14], inclusion of only U_{eff} cannot produce an insulating state even for large values such as $U_{\text{eff}} = 8$ eV, which is already beyond a reasonable value for this system. Therefore, we add to the LSDA + U approach the effects of SOC in the magnetization direction along the c axis, which is the high symmetry direction in the crystal structure. In the t_{2g} manifold, SOC transforms $\{d_{xy}, d_{yz}, d_{xz}\}$ into $\{d_{xy}, d_{\pm 1} = d_{xz} \pm i d_{yz}\}$ [11]. In the LSDA + SOC + U calculations, an energy gap appears at the critical value $U^c_{\text{eff}} \approx 3.7$ eV [24], and finally reaches the experimentally observed gap of ~0.4 eV at $U_{\text{eff}} = 5$ eV. Figure 1(c) shows the change in the energy gap as a function of U_{eff} in the C-AFM. The U^c_{eff} is somewhat larger than the value obtained from the constrained random-phase approximation [20], since U acts on the mixture of Cr $3d$ and O $2p$ due to the strong p-d hybridization, which can be measured in the DOS of Fig. 2. It is noteworthy that there is a regime around U^c_{eff} in which both metallic and insulating solutions are obtained, as is extensively discussed in literature [27]. However, for this system an insulating state is always energetically favored over a metallic state at the same U_{eff} in this regime.

To disclose the nature of the insulating state, we analyze the electronic and magnetic structures in detail. Figure 1(c) shows that the C-AFM is energetically favored over FM, which has a much lower energy than the nonmagnetic state (by 216 meV/f.u. in LSDA + SOC), regardless of the strength of U_{eff}. As U_{eff} increases, the difference in energy (ΔE) per formula unit between these two states monotonically decreases with a slope of $\Delta E / U_{\text{eff}} = -6.6 \times 10^{-3}$. Using a simple Heisenberg model $H = -J \sum_{i,j} \vec{S}_i \cdot \vec{S}_j$, for this spin $S = 1$ configuration the superexchange parameter J is estimated by $J = \Delta E \approx 42$ meV at $U_{\text{eff}} = 5$ eV. The C-AFM alignment has been observed in both $CaCrO_3$ and $SrCrO_3$ [15,17].

Now, we focus on the C-AFM alignment in both the metallic and insulating phases, where the latter is obtained from the LSDA + SOC + U calculations at $U_{\text{eff}} = 5$ eV. The total and atom-projected DOSs for both the metallic and insulating phases are displayed in Fig. 2. The corresponding band structures with the emphasized fatbands of the d_{xy} and

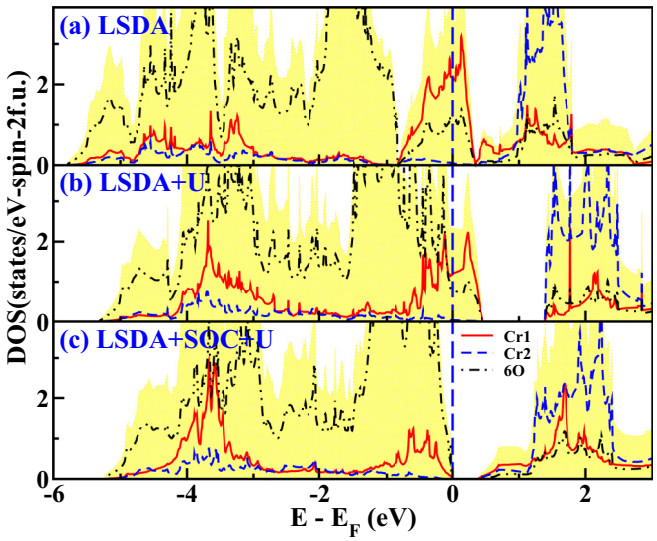

FIG. 2. (Color online) Atom-resolved densities of states (DOSs) for the spin-up channel in LSDA, LSDA + U, and LSDA + SOC + U (from top to bottom) in the C-AFM, containing two formula units. For LSDA + U and LSDA + U + SOC, $U_{\rm eff} = 5$ eV was used. The shaded region denotes the total DOS. In LSDA (and LSDA + SOC), the t_{2g}-e_g crystal field splitting is ∼1.5 eV, identical to the exchange splitting of the t_{2g} manifold. (The LSDA + SOC DOS, which is nearly identical to that of LSDA, is not shown here.)

the $d_{\pm1}$ orbitals are given in Fig. 3. In fact, the electronic structures of LSDA + SOC are nearly identical to those of LSDA (not shown here), since the strength of SOC is only several meV near the Fermi energy. In the metallic state, the partially filled t_{2g} manifold is separated from the unfilled e_g manifold in most regimes, but the d_{xy} band touches the bottom of the conduction band with a d_{z^2} character at the M point. As shown in the DOS, W of the $\frac{2}{3}$-filled t_{2g} manifold consistent

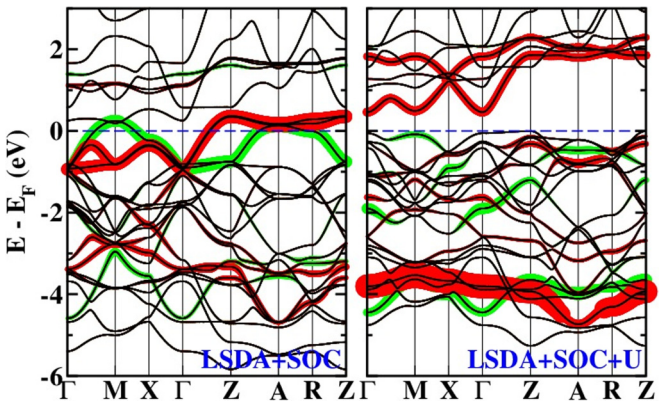

FIG. 3. (Color online) C-AFM band structures of LSDA + SOC (left) and LSDA + SOC + U at $U_{\rm eff} = 5$ eV (right), plotted in the basal plane. The highlighted fatbands indicate the d_{xy} (green color) and $d_{\pm1}$ (red color) characters of the spin-up Cr. As expected from the weak SOC strength, the LSDA + SOC band structure is nearly identical to that of LSDA (not shown here). In the 45° rotated supercell, the $X(A)$ and $M(R)$ points are $(\frac{\pi}{a},\frac{\pi}{a},\xi)$ and $(\frac{\pi}{a},0,\xi)$, respectively. ξ is zero for the first symbols and $\frac{\pi}{c}$ for the symbols in parentheses.

TABLE I. Individual spin M_S, orbital M_L, and net $M_{\rm net}$ moments of the C-AFM (in units of μ_B), obtained from LSDA + SOC and LSDA + SOC + U at $U_{\rm eff} = 5$ eV calculations. The moments of the planar oxygens are zero by symmetry.

	LSDA + SOC			LSDA + SOC + U		
Ion	M_S	M_L	$M_{\rm net}$	M_S	M_L	$M_{\rm net}$
Cr	1.677	−0.040	1.637	1.451	−0.781	0.670
Apical O	0.073	0.004	0.077	0.095	−0.075	0.020

with the d^2 configuration is about 1.3 eV. This leads to an estimated value of the nearest neighbor hopping parameter $t \approx 0.1$ eV. This value is half of that for the nonmagnetic state, indicating a considerable narrowing due to the AFM alignment. Our calculated moments are listed in Table I. The spin moment M_S for Cr is $1.68\mu_B$, substantially lower than the formal value of $2\mu_B$ due to the strong p-d hybridization. These features can be visualized in a spin-density isocountour plot, as displayed in the top panel of Fig. 4. In the metallic phase, the minority of Cr atoms has a $d_{z^2} + id_{x^2-y^2}$ character, while the majority of Cr indicates an equally occupied t_{2g} manifold. This clear visibility of the minority density indicates a strong $pd\sigma$ hybridization.

In the insulating state, the upper Hubbard band is at the bottom of the conduction band, while the occupied d_{xy} and the lower Hubbard band are mostly around −4 eV, as shown in the right panel of Fig. 3. The corresponding spin-density plot is displayed in the middle panel of Fig. 4. The Cr majority character represents a mixture of $d_{xy} + id_{\pm1}$. As given in Table I, the Cr orbital moment $M_L \approx -0.78\ \mu_B$ is antialigned to the corresponding M_S, leading to the net moment $M_{\rm net} = 0.67\mu_B$. This antialignment indicates that the lower Hubbard band has mostly the d_{-1} character for the spin-up Cr, but the d_{+1} character for the spin-down Cr. This zigzag OO in the ab plane is consistent with the C-AFM alignment. A similar OO was observed in the spinel ZnV_2O_4 as including both U and SOC [28,29]. Although some $3d$ systems show an unquenched M_L [30–36], this substantially large M_L is rare in $3d$ systems. Interestingly, the spin density of the apical oxygens clearly indicates the $p_x \pm ip_y$ character, even though the M_S of the apical oxygens is only $0.095\mu_B$. M_S of the apical oxygen is nearly compensated by the considerable $M_L = -0.075\mu_B$, which is unprecedented for an oxygen ion [31]. However, recently this unusual feature has been observed in a $5d$ system [37].

IV. DISCUSSION AND SUMMARY

We also performed LSDA + SOC + U calculations for our optimized volume. As expected from widening W of the t_{2g} manifold by ∼25% due to compression of the volume, in the optimized structure a gap appears at $U_{\rm eff}^c \approx 5.5$ eV, about 50% larger than in the experiment structure. Thus, if the optimized volume can be attained experimentally, this system would be metallic. These results suggest that change in strain (or applying a pressure) leads to an insulator-metal transition in this system.

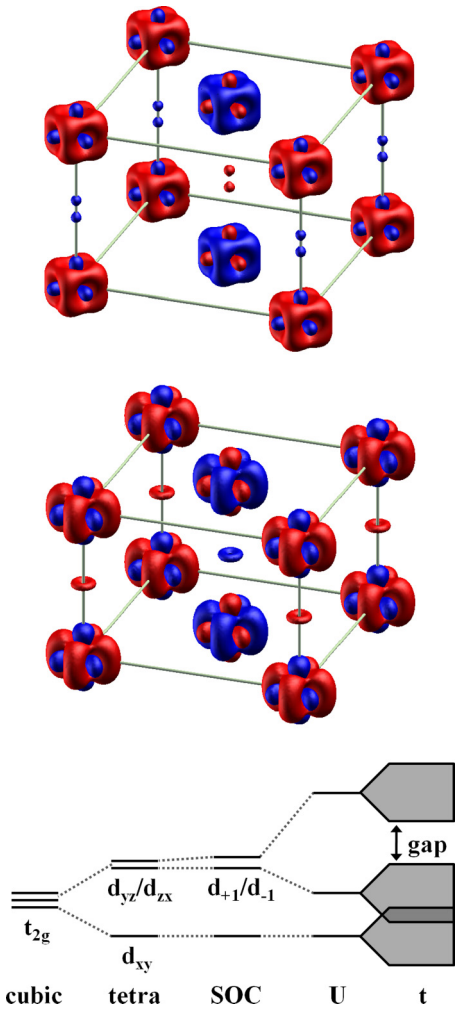

FIG. 4. (Color online) Spin density plots of Cr ions for LSDA + SOC (top) and LSDA + SOC + U (middle) in the $\sqrt{2} \times \sqrt{2}$ supercell. The isosurface of LSDA + SOC + U is at 0.063 $e/\text{Å}^3$, while a slightly larger isovalue of 0.1 $e/\text{Å}^3$ is used in LSDA + SOC for a better visualization. The spin density of the apical oxygens is clearly visible, while that of the planar oxygens is invisible for this isovalue. The different colors represent the opposite spin orientation in the C-AFM state. Bottom: schematic evolution of the spin-up t_{2g} manifold in the cubic symmetry, through tetragonal distortion, SOC, Coulomb repulsion U, and dispersion due to hopping t.

To investigate the stability of these structures, we carried out linear response full-phonon calculations for both the experiment volume and our optimized volume. The results are displayed in Fig. 5. In good agreement with the instability in the bulk [14], there are several imaginary frequencies in the experiment volume. However, our results show that in the optimized volume both the tetragonal and cubic perovskites are stable. This suggests that these phases would be achieved

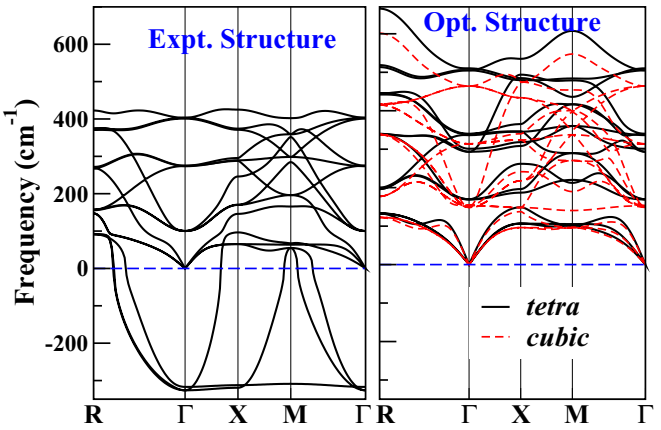

FIG. 5. (Color online) GGA phonon spectra with the experimental (left) and our optimized volumes (right). The experimental spectrum shows imaginary frequencies throughout all regimes, indicating a significant instability in structure.

by a proper choice of substrate or a high pressure technique, requiring further experiments. Considering the tiny difference in energy ($\leqslant$1 meV) between the cubic and the tetragonal phases, our results imply that the cubic structure would be stabilized by quantum fluctuations [38].

In summary, we have carried out *ab initio* calculations including both correlation and SOC effects to investigate a tetragonally distorted perovskite $BaCrO_3$, the volume of which seems to be considerably enhanced by the strain of the $SrTiO_3$ substrate. Inclusion of both SOC and U causes this d^2 system to change to insulating at $U^c_{\text{eff}} \approx 3.7$ eV, though the metallic state remains unchanged on applying U only. This indicates a crucial role of SOC in this Mott insulator, which is uncommon in 3d systems. In the insulating state, one electron occupies d_{xy} and the other alternatively occupies $d_{xz} + id_{yz}$ or $d_{xz} - id_{yz}$ orbital, resulting in an unquenched Cr orbital moment M_L which is antialigned to the Cr spin moment $M_S \approx 2|M_L|$. This is consistent with the ground state of C-AFM, implying that the observed small moment is due to a little canted spin. Remarkably, due to the spin and orbital orderings of the Cr ions the spin density of the apical oxygen ions clearly shows the admixture of $p_x \pm ip_y$ characters, leading to the considerable spin and orbital moments antialigned to each other. These may be directly probed by further experiments like x-ray resonant spectroscopy.

ACKNOWLEDGMENTS

We acknowledge C. Kim for useful discussions on a thin film growth, W. E. Pickett and D. Kashinathan for useful communications on an OO, and H. B. Rhee for a critical reading of the manuscript. This research was supported by NRF-2013R1A1A2A10008946 (Korea).

[1] J. Mannhart and D. G. Schlom, Science **327**, 1607 (2010).

[2] H. Y. Hwang, Y. Iwasa, M. Kawasaki, B. Keimer, N. Nagaosa, and Y. Tokura, Nat. Mater. **11**, 103 (2012).

[3] W. Witczak-Krempa, G. Chen, Y. B. Kim, and L. Balents, Annu. Rev. Condens. Matter Phys. **5**, 57 (2014).

[4] C.-G. Duan, R. F. Sabiryanov, J. Liu, W. N. Mei, P. A. Dowben, and J. R. Hardy, Phys. Rev. Lett. **94**, 237201 (2005).

[5] J. Chaloupka and G. Khaliullin, Phys. Rev. Lett. **100**, 016404 (2008).

[6] M. Ziese, H. C. Semmelhack, and K. H. Han, Phys. Rev. B **68**, 134444 (2003).

[7] J. Wang, F. X. Hu, R. W. Li, J. R. Sun, and B. G. Shen, Appl. Phys. Lett. **96**, 052501 (2001).

[8] S. Tan, Y. Zhang, M. Xia, Z. Ye, F. Chen, X. Xie, R. Peng, D. Xu, Q. Fan, H. Xu, J. Jiang, T. Zhang, X. Lai, T. Xiang, J. Hu, B. Xie, and D. Feng, Nat. Mater. **12**, 634 (2013).

[9] E. S. Reich, Nature (London) **501**, 474 (2013).

[10] H.-S. Kim, C. H. Kim, H. Jeong, H. Jin, and J. Yu, Phys. Rev. B **87**, 165117 (2013).

[11] K.-W. Lee and W. E. Pickett, Europhys. Lett. **80**, 37008 (2007).

[12] B. J. Kim, H. Jin, S. J. Moon, J. Y. Kim, B. G. Park, C. S. Leem, J. Yu, T. W. Noh, C. Kim, S. J. Oh, J. H. Park, V. Durairaj, G. Cao, and E. Rotenberg, Phys. Rev. Lett. **101**, 076402 (2008).

[13] Y. Luo, C. Cao, B. Si, Y. Li, J. Bao, H. Guo, X. Yang, Ch. Shen, Ch. Feng, J. Dai, G. Cao, and Z. A. Xu, Phys. Rev. B **87**, 161121(R) (2013).

[14] Z. H. Zhu, F. J. Rueckert, J. I. Budnick, W. A. Hines, M. Jain, H. Zhang, and B. O. Wells, Phys. Rev. B **87**, 195129 (2013).

[15] J.-S. Zhou, C.-Q. Jin, Y.-W. Long, L.-X. Yang, and J. B. Goodenough, Phys. Rev. Lett. **96**, 046408 (2006).

[16] A. C. Komarek, S. V. Streltsov, M. Isobe, T. Moller, M. Hoelzel, A. Senyshyn, D. Trots, M. T. Fernández-Díaz, T. Hansen, H. Gotou, T. Yagi, Y. Ueda, V. I. Anisimov, M. Gruninger, D. I. Khomskii, and M. Braden, Phys. Rev. Lett. **101**, 167204 (2008).

[17] L. Ortega-San-Martin, A. J. Williams, J. Rodgers, J. P. Attfield, G. Heymann, and H. Huppertz, Phys. Rev. Lett. **99**, 255701 (2007).

[18] K.-W. Lee and W. E. Pickett, Phys. Rev. B **80**, 125133 (2009).

[19] K. Gupta, P. Mahadevan, Ph. Mavropoulos, and M. LeŽaić, Phys. Rev. Lett. **111**, 077601 (2013).

[20] G. Giovannetti, M. Aichhorn, and M. Gapone, arXiv:1402.0901.

[21] K. Schwarz and P. Blaha, Comput. Mater. Sci. **28**, 259 (2003).

[22] W. E. Pickett and D. J. Singh, Phys. Rev. B **53**, 1146 (1996).

[23] P. Giannozzi, S. Baroni, N. Bonini, M. Calandra, R. Car, C. Cavazzoni, D. Ceresoli, G. L. Chiarotti, M. Cococcioni, I. Dabo, A. Dal Corso, S. Fabris, G. Fratesi, S. de Gironcoli, R. Gebauer, U. Gerstmann, C. Gougoussis, A. Kokalj, M. Lazzeri, L. Martin-Samos, N. Marzari, F. Mauri, R. Mazzarello, S. Paolini, A. Pasquarello, L. Paulatto, C. Sbraccia, S. Scandolo, G. Sclauzero, A. P. Seitsonen, A. Smogunov, P. Umari, and R. M. Wentzcovitch, J. Phys.: Condens. Matter **21**, 395502 (2009).

[24] As including U, we used two popular double counting schemes of the so-called around mean field (AMF) [25] and the fully localized limit (FLL) [26]. However, in the LSDA + SOC + U calculations, only the AMF scheme leads to open a gap above U^c_{eff}. This is consistent with the fact that AMF is often more suitable than FLL for the moderately correlated systems, as discussed in detail in literature [27]. Thus we will address the results from AMF here.

[25] V. I. Anisimov, I. V. Solovyev, M. A. Korotin, M. T. Czyzyk, and G. A. Sawatzky, Phys. Rev. B **48**, 16929 (1993).

[26] M. T. Czyzyk and G. A. Sawatzky, Phys. Rev. B **49**, 14211 (1994).

[27] K.-W. Lee, J. Kuneš, P. Novak, and W. E. Pickett, Phys. Rev. Lett. **94**, 026403 (2005).

[28] O. Tchernyshyov, Phys. Rev. Lett. **93**, 157206 (2004).

[29] T. Maitra and R. Valentí, Phys. Rev. Lett. **99**, 126401 (2007).

[30] S. K. Kwon and B. I. Min, Phys. Rev. B **62**, 73 (2000).

[31] D. J. Huang, H.-T. Jeng, C. F. Chang, G. Y. Guo, J. Chen, W. P. Wu, S. C. Chung, S. G. Shyu, C. C. Wu, H.-J. Lin, and C. T. Chen, Phys. Rev. B **66**, 174440 (2002).

[32] D. J. Huang, C. F. Chang, H.-T. Jeng, G. Y. Guo, H.-J. Lin, W. B. Wu, H. C. Ku, A. Fujimori, Y. Takahashi, and C. T. Chen, Phys. Rev. Lett. **93**, 077204 (2004).

[33] H. Wu, M. W. Haverkort, Z. Hu, D. I. Khomskii, and L. H. Tjeng, Phys. Rev. Lett. **95**, 186401 (2005).

[34] S. Sarkar, M. De Raychaudhury, I. Dasgupta, and T. Saha-Dasgupta, Phys. Rev. B **80**, 201101(R) (2009).

[35] S. Sarkar, T. Maitra, R. Valentí, and T. Saha-Dasgupta, Phys. Rev. Lett. **102**, 216405 (2009).

[36] J. Bartolomé, F. Bartolomé, L. M. García, G. Filoti, T. Gredig, C. N. Colesniuc, I. K. Schuller, and J. C. Cezar, Phys. Rev. B **81**, 195405 (2010).

[37] K.-H. Ahn, K.-W. Lee, and W. E. Pickett (unpublished).

[38] W. Zhong and D. Vanderbilt, Phys. Rev. Lett. **74**, 2587 (1995); Phys. Rev. B **53**, 5047 (1996).